International Journal of Mass Spectrometry 305 (2011) 138–150

Contents lists available at ScienceDirect

International Journal of Mass Spectrometry

journal homepage: www.elsevier.com/locate/ijms

Rapid profiling of bovine and human milk gangliosides by matrix-assisted laser desorption/ionization Fourier transform ion cyclotron resonance mass spectrometry

Hyeyoung Lee[a], Hyun Joo An[b], Larry A. Lerno Jr.[b], J. Bruce German[a,c,*,1], Carlito B. Lebrilla[b,d,**,1]

[a] Department of Food Science and Technology, University of California, Davis, CA 95616, United States
[b] Department of Chemistry, University of California, Davis, CA 95616, United States
[c] Nestle Research Center, Lausanne, Switzerland
[d] Department of Biochemistry and Molecular Medicine, University of California, Davis, CA 95616, United States

ARTICLE INFO

Article history:
Received 31 July 2010
Received in revised form 9 October 2010
Accepted 14 October 2010
Available online 30 October 2010

Keywords:
Ganglioside
Bovine milk
Human milk
Matrix-assisted laser desorption/ionization
Fourier transform ion cyclotron resonance
Kendrick mass defect

ABSTRACT

Gangliosides are anionic glycosphingolipids widely distributed in vertebrate tissues and fluids. Their structural and quantitative expression patterns depend on phylogeny and are distinct down to the species level. In milk, gangliosides are exclusively associated with the milk fat globule membrane. They may participate in diverse biological processes but more specifically to host–pathogen interactions. However, due to the molecular complexities, the analysis needs extensive sample preparation, chromatographic separation, and even chemical reaction, which makes the process very complex and time-consuming. Here, we describe a rapid profiling method for bovine and human milk gangliosides employing matrix-assisted desorption/ionization (MALDI) Fourier transform ion cyclotron resonance (FTICR) mass spectrometry (MS). Prior to the analyses of biological samples, milk ganglioside standards GM3 and GD3 fractions were first analyzed in order to validate this method. High mass accuracy and high resolution obtained from MALDI FTICR MS allow for the confident assignment of chain length and degree of unsaturation of the ceramide. For the structural elucidation, tandem mass spectrometry (MS/MS), specifically as collision-induced dissociation (CID) and infrared multiphoton dissociation (IRMPD) were employed. Complex ganglioside mixtures from bovine and human milk were further analyzed with this method. The samples were prepared by two consecutive chloroform/methanol extraction and solid phase extraction. We observed a number of differences between bovine milk and human milk. The common gangliosides in bovine and human milk are 2NeuAc–2Hex–Cer (GD3) and NeuAc–2Hex–Cer (GM3); whereas, the ion intensities of ganglioside species are different between two milk samples. Kendrick mass defect plot yields grouping of ganglioside peaks according to their structural similarities. Gangliosides were further probed by tandem MS to confirm the compositional and structural assignments. We found that only in human milk ganglioside was the ceramide carbon always even numbered, which is consistent with the notion that differences in the oligosaccharide and the ceramide moieties confer to their physiological distinctions.
Published by Elsevier B.V.

1. Introduction

Gangliosides are widely distributed in tissues and fluids of the vertebrate. As the components of cell membranes, they participate in diverse biological processes, including host–pathogen interactions, cell–cell recognition, and modulation of membrane protein function [1]. The biological roles of gangliosides are dependent on their two basic components: the ceramide lipid chain and the anionic oligosaccharide moiety that has one or more sialic acids (or N-acetylneuraminic acid, NeuAc). In the ceramide moiety, a fatty acid is linked to a sphingoid base. The oligosaccharide headgroup is attached at the primary hydroxyl of the ceramide chain [1,2]. In milk, gangliosides are almost exclusively associated with the milk fat globule membrane (MFGM), where the oligosaccharide may interact with the external environment, while the ceramide

Abbreviations: MALDI, Matrix-assisted laser desorption/ionization; FTICR, Fourier transform ion cyclotron resonance; CID, Collision-induced dissociation; IRMPD, Infrared multiphoton dissociation; MFGM, Milk fat globule membrane; KMD, Kendrick mass defect; KNM, Kendrick nominal mass; NeuAc, N-acetylneuraminic acid; Hex, Hexose; HexNAc, N-acetylhexosamine.

* Corresponding author at: Department of Food Science and Technology, University of California, Davis, CA 95616, United States. Tel.: +1 530 752 1486; fax: +1 530 752 4759.
** Corresponding author at: Department of Chemistry, University of California, Davis, CA 95616, United States. Tel.: +1 530 752 0504; fax: +1 530 752 8995.
E-mail addresses: jbgerman@ucdavis.edu (J.B. German), cblebrilla@ucdavis.edu (C.B. Lebrilla).
[1] J. Bruce German and Carlito B. Lebrilla equally contributed to this paper as co-corresponding authors.

1387-3806/$ – see front matter. Published by Elsevier B.V.
doi:10.1016/j.ijms.2010.10.020

is anchored into the membrane to act as an intracellular regulator upon binding with external components [3,4]. Milk directs and regulates the immune, metabolic, and microflora systems of the infant. It enhances nutrient absorption and delivery while conferring multiple means of protection for the maternal mammary epithelia and the infant gastrointestinal system [5]. Furthermore, because gangliosides are derived mainly from the apical plasma membrane of the epithelial cells in the lactating mammary gland, they may contribute to the prevention of infection and to immunity [6–9]. Therefore, knowledge of both the oligosaccharide and the ceramide structures can provide the necessary insight into the physiological roles and effects of milk gangliosides that may vary among species.

Because of their amphipathic nature and structural complexity, the classical methods using multiple chromatographic analyses along with the release of the individual components require extensive sample preparation. Moreover, the methods provide only partial information yielding either the oligosaccharide or the ceramide portion. Glycan headgroups of milk gangliosides have been analyzed by thin layer chromatography (TLC) and were identified by either comparing the retention factor with standard gangliosides or using antibody for the specific detection [10,11]. Ceramide moieties were elucidated through several steps including derivatization, solvent extraction, and gas chromatography analysis. To profile ceramide heterogeneity of each ganglioside species, the designated TLC spot would be collected prior to ceramide analysis [10,12,13]. Consequently, the complete analytical flow has become very complex and laborious. The methods often fail to describe in precise details both the ceramide and glycan moieties simultaneously [14,15]. Therefore, developments in novel rapid analytical methods, including mass spectrometry (MS), have been necessary in addressing the complexity of milk gangliosides.

Matrix-assisted laser desorption/ionization (MALDI) has emerged as a tool for the analysis of carbohydrate and glycoconjugates. Most carbohydrates produce signals in their native state providing compositional and structural information [16,17]. However, glycoconjugates containing sialic acid have been examined very carefully due to the loss of labile sialic acid during the ionization process. Derivatization such as methylation, as well as permethylation in general, increases the sensitivity and stability of the gangliosides; however, it may not yield complete stabilization [18–20]. Moreover, additional preparation steps can result in the losses of the gangliosides, which often exists in trace amounts in biological samples.

Many studies have been performed using MALDI with combination of Time-of-Flight (TOF) for ganglioside analysis [14,18,21,22]. However, the TOF analyzers in this configuration have limited mass resolution making it difficult to examine mixtures when they are close in mass. High-resolution mass analyzers are becoming more necessary for assigning complex polar lipids that have variations not only in subclasses but also in the number of double bonds and hydroxylation in their backbone structures [23,24]. Several reports have described the use of MALDI FTICR MS for the analysis of gangliosides. Penn et al. examined several parameters affecting ganglioside analysis [19]. O'Connor et al. employed a high-pressure MALDI source to improve molecular ion yields of fragile gangliosides using collision cooling [25,26]. This analytical method was further applied to brain ganglioside analysis in combination with thin layer chromatography [27]. Oligosaccharide sequences, branching patterns, and linkage information as well as ceramide composition of gangliosides were determined by tandem mass spectrometry (MS/MS) [28–30].

In this study, we describe a rapid, accurate method for profiling glycan and lipid components of ganglioside mixtures. Native bovine milk ganglioside GM3 and GD3 fractions were analyzed to validate the experimental conditions. Measured accurate mass values combined with Kendrick mass defect plot reveals each compound's oligosaccharide headgroup and the carbon distribution in ceramide backbone. The assignments were confirmed and further structural information was obtained using tandem MS.

2. Experimental

2.1. Materials

Sodium chloride and 2,5-dihydroxybenzoic acid (DHB) were purchased from Sigma–Aldrich (St. Louis, MO). DEAE–Sephadex resin was obtained from GE Health Care Bio-Sciences (Little Chalfont, UK), and C18 solid phase extraction (SPE) cartridges, 500 mg in a syringe barrel with 3 mL reservoir, were obtained from Supelco (Bellefonte, PA). Bovine buttermilk gangliosides GM3 (NeuAcα2–3Galβ1–4Glcβ–Cer) and GD3 (NeuAcα2–8NeuAcα2–3Galβ1–4Glcβ–Cer) were purchased from Matreya (Pleasant Gap, PA). All solvents used for this study were of analytical or HPLC grade.

Bovine milk was obtained from the dairy at the University of California, Davis. Human milk samples were obtained from the Foods for Health Institute's lactation program, which has established collaborations with various lactation centers (University of Reno and University of California Davis). Collected bovine and human milk samples were pooled and frozen at −80 °C. They were thawed prior to sample preparation.

2.2. Nomenclature

The abbreviated nomenclature for the gangliosides follows the system of Svennerholm [31], which is based on the oligosaccharide structure. The composition of a ceramide portion is defined by a formula, e.g., d41:1, where d refers the dihydroxy sphingoid base, the first figure to the sum of carbon atoms, and the second to the number of double bonds in the ceramide. Fragmentations are assigned according to the nomenclature for carbohydrate fragmentation by Domon and Costello [32].

2.3. Sample preparation

Stock solutions of the standards were prepared at the concentration of 1 mg/mL, and subsequently stored at −20 °C. Ganglioside extraction proceeded as previously described with minor modifications [33,34]. Briefly, homogenized milk samples were mixed with chloroform/methanol (1:2, v/v) and centrifuged, and the aqueous upper layer was collected. The pellet was washed with the chloroform/methanol (1:2, v/v) for the complete extraction. The aqueous layers were combined, dried under the vacuum, and partitioned again with chloroform/methanol (2:1, v/v). The gangliosides were then enriched by DEAE-Sephadex anion exchange column and C18 solid phase extraction. The ganglioside mixtures were solubilized in methanol prior to mass spectrometry analysis. The concentrations of working solutions ranged from 0.5 mg/mL to 0.01 mg/mL.

2.4. Matrix-assisted laser desorption/ionization Fourier transform ion cyclotron resonance mass spectrometry

All experiments were performed on an IonSpec Pro MALDI FTICR MS (IonSpec, Irvine, CA) equipped with a 7.0 T superconducting magnet. A pulsed Nd:YAG laser (355 nm) was used as the external MALDI source. Ganglioside samples were co-spotted on a disposable MALDI plate (Hudson Surface technology, Inc., Newark, NJ) with a matrix to produce gas-phase ions in either the positive or negative ion mode. 2,5-Dihydroxybenzoic acid (DHB) was chosen as a matrix based on previous findings [19,27]. The matrix solution contained 50 mg/mL DHB in 50% acetonitrile in water. For the pos-

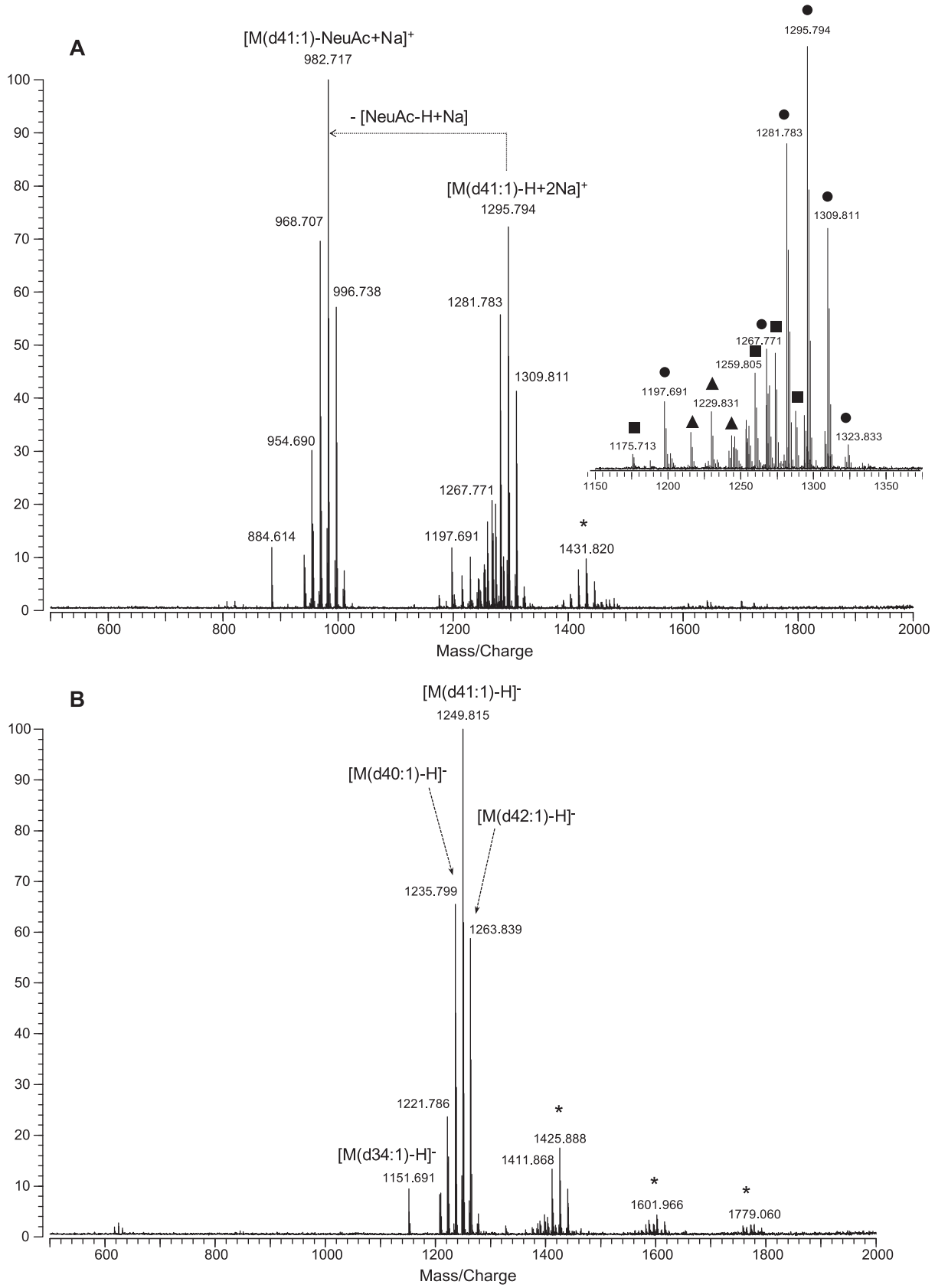

Fig. 1. MALDI-MS spectra of ganglioside GM3 from bovine buttermilk in (A) positive- and (B) negative ion detection mode. Zoom-in spectrum is shown in the inset. Symbols for the types of quasimolecular ions: (●) $[M-H+2Na]^+$; (■) $[M+Na]^+$; (▲) $[M-CO_2+Na]^+$. Asterisk (*) denotes that matrix–ganglioside adducts are detected with low abundance.

itive ion mode, 0.01 M NaCl was added as a cation dopant. 1 μL of ganglioside was applied to the probe tip, followed by 0.5 μL of NaCl solution in 50% acetonitrile in water, followed by 1 μL of matrix. For the negative ion spectra, the DHB matrix was used without dopant. The samples were mixed on the probe surface and dried under vacuum prior to analysis.

Ions were desorbed from the sample target plate by 5–20 laser shots. Laser power was adjusted slightly above the ion formation threshold to obtain minimal in-source fragmentation and sufficient signal intensity [19]. Ions were accumulated in a hexapole and then injected into the cylindrical ICR cell via an RF-only quadrupole ion guide. In the cell, the trapped ions were excited by a sweep of RF frequencies and detected in the *m/z* range of 220–4500. Transients were acquired using IonSpec OMEGA software. Frequency domain mass spectra were obtained by the fast Fourier transformation of a 1.024-s transient signal acquired using an ADC rate of 1 MHz. Mass spectra were firstly calibrated with the use of maltooligosaccharides for external calibration, and then two ganglioside peaks whose composition had been confirmed by MS/MS experiments were chosen for internal calibration [35].

2.5. Tandem mass spectrometry

Tandem MS analysis was achieved via collision-induced dissociation (CID) and infrared multiphoton dissociation (IRMPD). Prior to performing tandem MS, the ion of interest was isolated in the ICR cell by the use of arbitrary waveform generation and synthesizer excitation. CID experiments were performed in the off-resonance mode. The isolated ions were excited at a frequency 1000 Hz greater than the effective cyclotron frequency for 500 ms at 3–4 $V_{b\text{-}p}$. The isolation event is then followed by an introduction of a pulse of nitrogen gas into the ICR cell to collisionally activate the isolated ions. For IRMPD, a 10.6 μm carbon dioxide laser (Parallax Laser, Waltham, MA) provided IR photons (0.1 eV per photon), which were directed into the ICR cell through an IR-transparent window composed of BaF_2 (Bicron, Newbury, OH). The laser beam diameter was 6 mm, expanded to 12 mm by means of a 2× beam expander (Synrad, Mukilteo, WA) to accommodate the dispersed ion cloud. Photon irradiation was performed between 7 and 7.5 s for the duration of 1.5 s with beam attenuation set to pass 70% of 20 W maximum power.

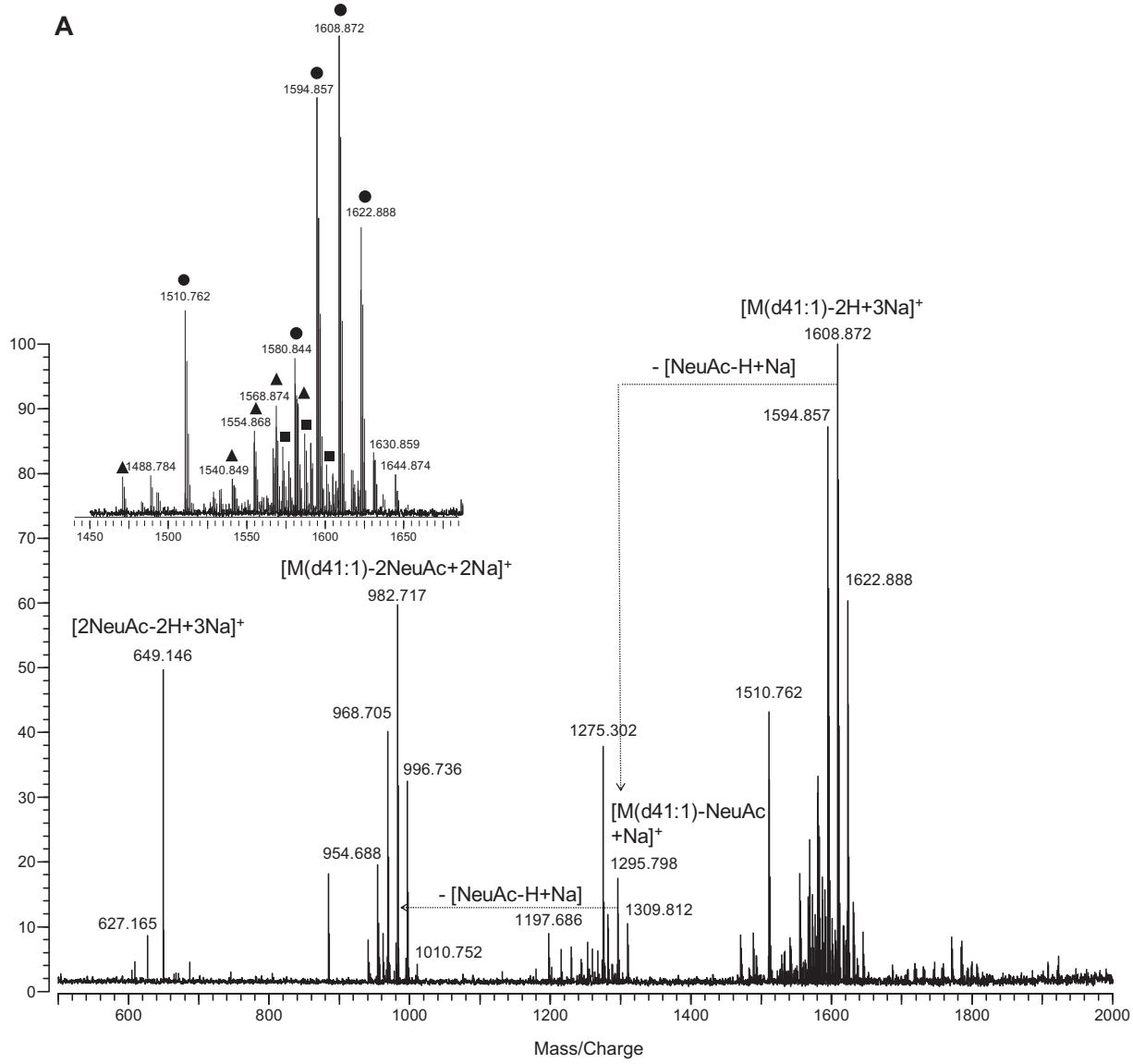

Fig. 2. MALDI-MS spectra of ganglioside GD3 from bovine buttermilk in (A) positive- and (B) negative ion detection mode. Symbols for the types of quasimolecular ions: (●) $[M-2H+3Na]^+$; (■) $[M-H+2Na]^+$; (▲) $[M-H-H_2O+2Na]^+$; (○) $[M-H]^-$; (□) $[M+Na-2H]^-$; (△) $[M-H_2O-H]^-$.

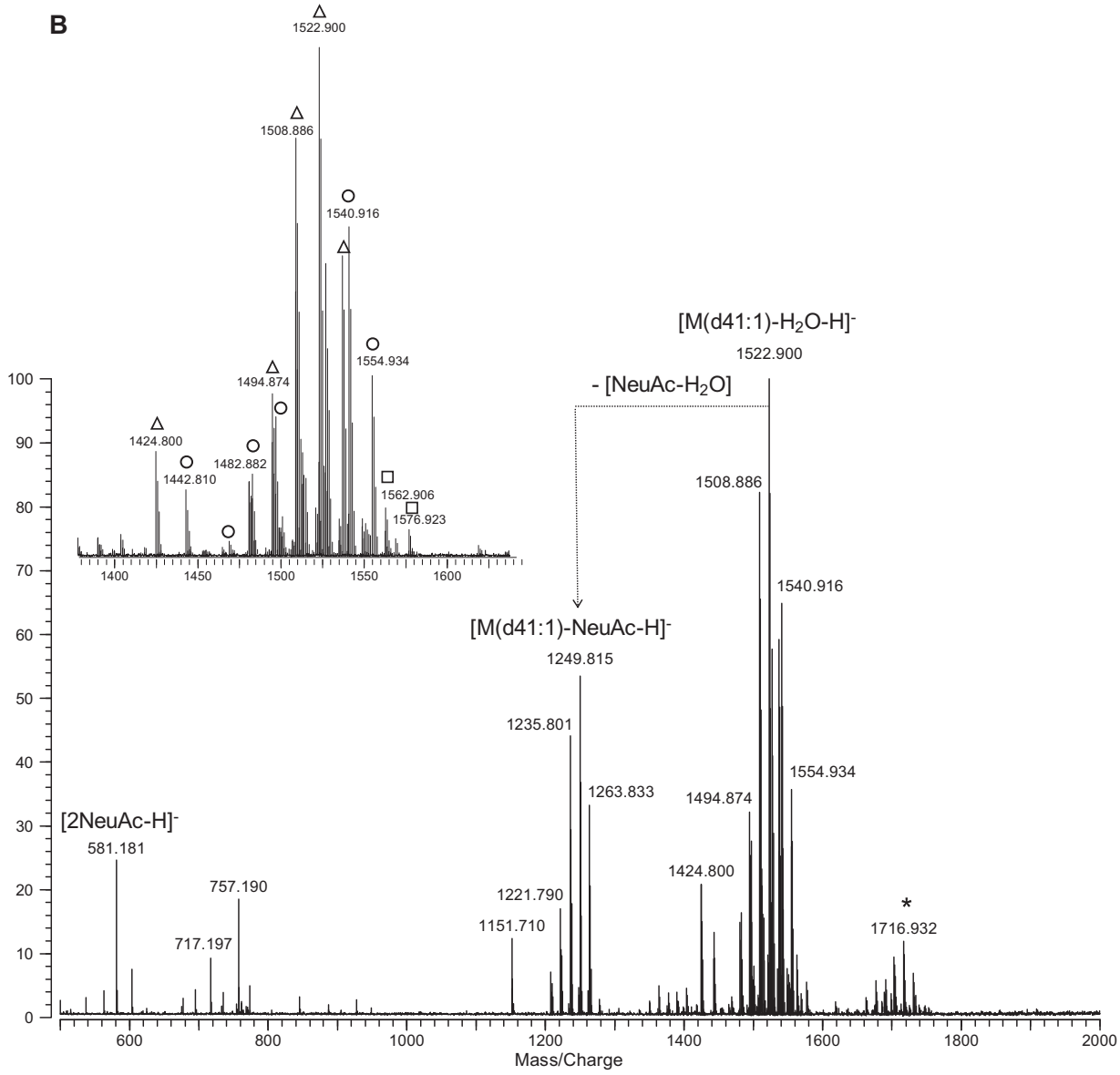

Fig. 2. (*Continued*).

2.6. Kendrick mass defect (KMD)

Kendrick mass defect analysis was performed on the data sets with the purpose of aiding in the rapid identification of the gangliosides. This method scales all the measured *m/z* values relative to the *m/z* of CH_2, which is defined as exactly 14.00000. Therefore, in the expression of the masses of gangliosides differing by one or more CH_2 in the Kendrick mass scale, all homologous molecules will have the same Kendrick mass defect, and the adjacent ions in a homologous series will be separated by 14.00000. The Kendrick masses are further processed to Kendrick mass defects, which are the differences between the exact Kendrick mass and the nominal Kendrick mass (NKM), which is the nearest integer mass. The KMD represents the different types and numbers of heteroatoms in the molecules, and the NKM represents the length of repeating CH_2. For the visualization of the Kendrick mass data sets, two-dimensional plots of KMDs as a function of NKM are displayed. Members of a homologous CH_2 are horizontally aligned according to the KMD of the series, but compounds with different heteroatoms are located on distinct vertical regions. Plotting the data in this manner reveals identifying trends, which are useful for the rapid data analysis [36].

The procedure was performed as follows. First, all mass values for ions of *m/z* 1000–2000 and greater than 7% of relative abundance were imported to a Microsoft Excel 2007 datasheet. The measured masses were then converted from the IUPAC mass scale to the Kendrick mass scale by the multiplication of the mass values with 14.00000/14.01565, in which the mass of the CH_2 is taken as integer 14 mass units [37]. KMD was calculated by the subtraction of NKM from the Kendrick mass. Afterwards the calculated NKM and KMD were plotted and displayed.

3. Results and discussion

Prior to the analyses of biological sample, we optimized and validated the method for optimal sensitivity and to avoid misidentification. Standard gangliosides from bovine milk (GM3 and GD3) were examined first.

3.1. MS analysis of ganglioside GM3 and GD3 standards from bovine milk

In this study, two common milk gangliosides, monosialoganglioside GM3 and disialoganglioside GD3 standards were analyzed under conditions described in Section 2. In the positive ion mode (Fig. 1A), all observed GM3 ganglioside ions corresponded to the sodium-coordinated species such as $[M-H+2Na]^+$, $[M+Na]^+$ and $[M-CO_2+Na]^+$. The di-sodiated $[M-H+2Na]^+$ species of the GM3 likely arise from the exchange of the carboxylic acid proton with a sodium. MALDI FTICR MS of gangliosides were previously shown to yield significant fragmentation [19]. To profile gangliosides, it is important to control the fragmentation. The base peak in the spectrum corresponds to the fragment ion $[M(d41:1)-NeuAc+Na]^+$ at *m/z* 982.717, which results from the loss of sialic acid from $[M(d41:1)-H+2Na]^+$ at *m/z* 1295.794. Sialic acids are highly labile, and during MS analysis sialic acid losses often occur particularly in the positive mode. In each of the two peak clusters, the molecular ions and the ions from sialic losses, series of ions which have 14 Da mass difference, corresponding to CH_2, and 2 Da difference from compound series differing in the number of double bonds were observed indicating the heterogeneities in the ceramide backbone structures. In contrast to the abundance of adduct species in the positive ion mode, the negative ion mode spectrum (Fig. 1B) yielded only deprotonated ions ($[M-H]^-$). Moreover, as anionic species, they provide better signal to noise ratios in the negative mode compared to the positive mode. Major GM3 species were composed of 34, 39, 40, 41, and 42 carbons with double bonds ranging from 0 to 2 in their ceramide portions (Suppl. 1). Interestingly, we observe up to three non-covalent DHB matrix adductions, which were reported under high pressure collision cooling conditions by Costello's group [25,26].

GD3 shows multiple cationized species including di-sodiated ($[M-H+2Na]^+$ and $[M-H-H_2O+2Na]^+$) and tri-sodiated ($[M-2H+3Na]^+$) (Fig. 2A). An intact disialoganglioside peak corresponding to $[M(d41:1)-2H+3Na]^+$ at *m/z* 1608.872 was observed as a base peak under this experimental condition. In the negative ion mode, three different types of molecular ions were observed, $[M-H_2O-H]^-$, $[M-H]^-$ and $[M+Na-2H]^-$, yielding a more complicated spectrum than that of GM3 (Fig. 2B). In both ion modes, loss of a water molecule from the molecular ions was observed, which indicates that the sialic acids that are α2,3 linked can generate internal esters, known as lactones, between the carboxyl groups of the sialic acid residues and a hydroxyl group on the galactose residues [18]. Disialogangliosides GD1a (NeuAcα2–3Galβ1–3GalNAcβ1–4(NeuAcα2–3)Galβ1–4Glcβ–Cer) and GD1b (Galβ1–3GalNAcβ1–4(NeuAcα2–8NeuAcα2–3)Galβ1–4Glcβ–Cer) have been shown to exhibit this behavior in MALDI ionization spectra [18,19]. GD3 with ceramide types d34:1, d39:1, d40:1, d41:1, and d42:1 were abundant in bovine buttermilk with minor variation in the degree of unsaturation observed (Suppl. 2). The ceramide composition was similar to that of GM3, indicating that bovine milk gangliosides originate from a common pool of ceramide [2]. Two abundant ions at *m/z* 649.146 ($[2NeuAc-2H+3Na]^+$) and at *m/z* 581.181 ($[2NeuAc-H]^-$) indicate that two sialic acids are bound and located at the terminal position.

3.2. Structure elucidation of gangliosides by tandem MS using collision induced dissociation (CID) and infrared multiphoton dissociation (IRMPD)

Tandem MS has been widely applied to the structural investigation of glycoconjugates including free oligosaccharides,

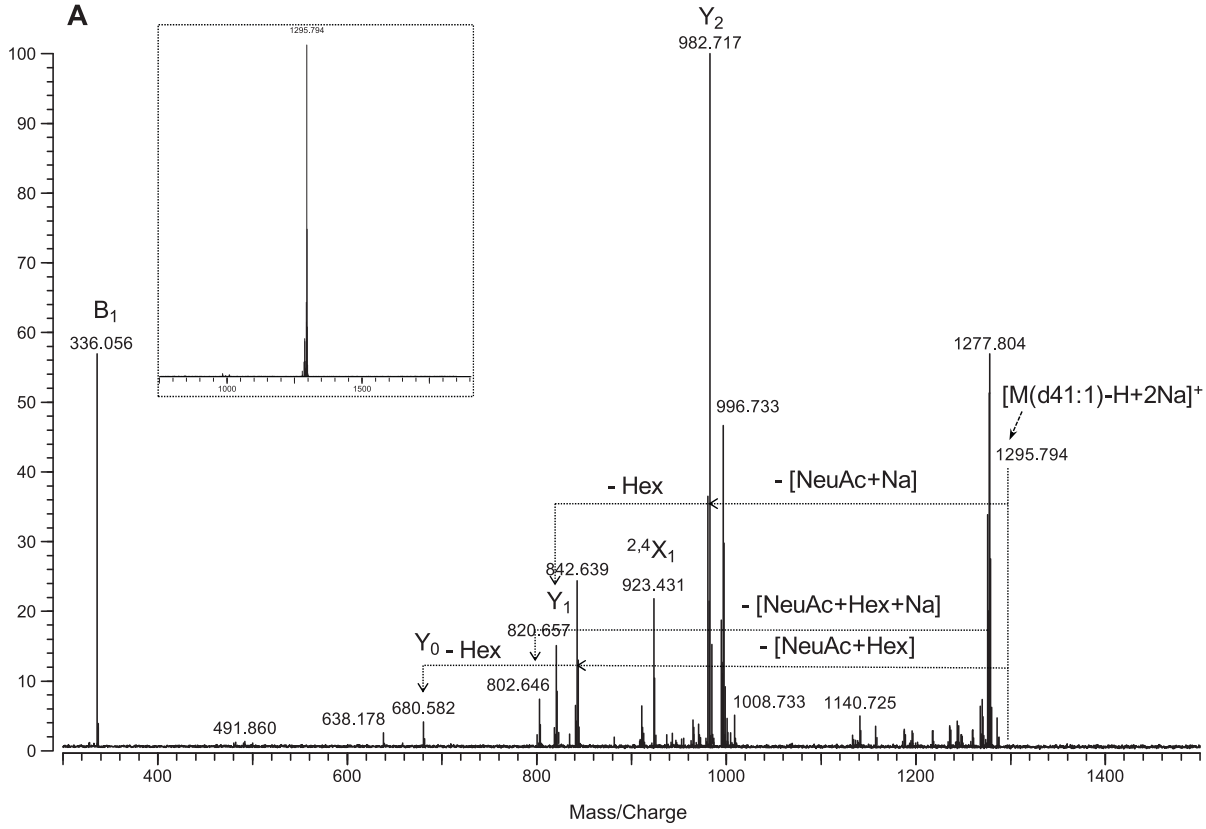

Fig. 3. Tandem MS spectra of ganglioside GM3 from bovine buttermilk in the positive mode using (A) CID and (B) IRMPD with the precursor ion at *m/z* 1295.794. Insets are the isolation of the peak of interest. (C) Fragmentation by tandem MS of the GM3 species. The structure depicted refers to GM3, the dominant form in bovine milk. The assignment of fragment ions is according to the nomenclature of Domon and Costello [32].

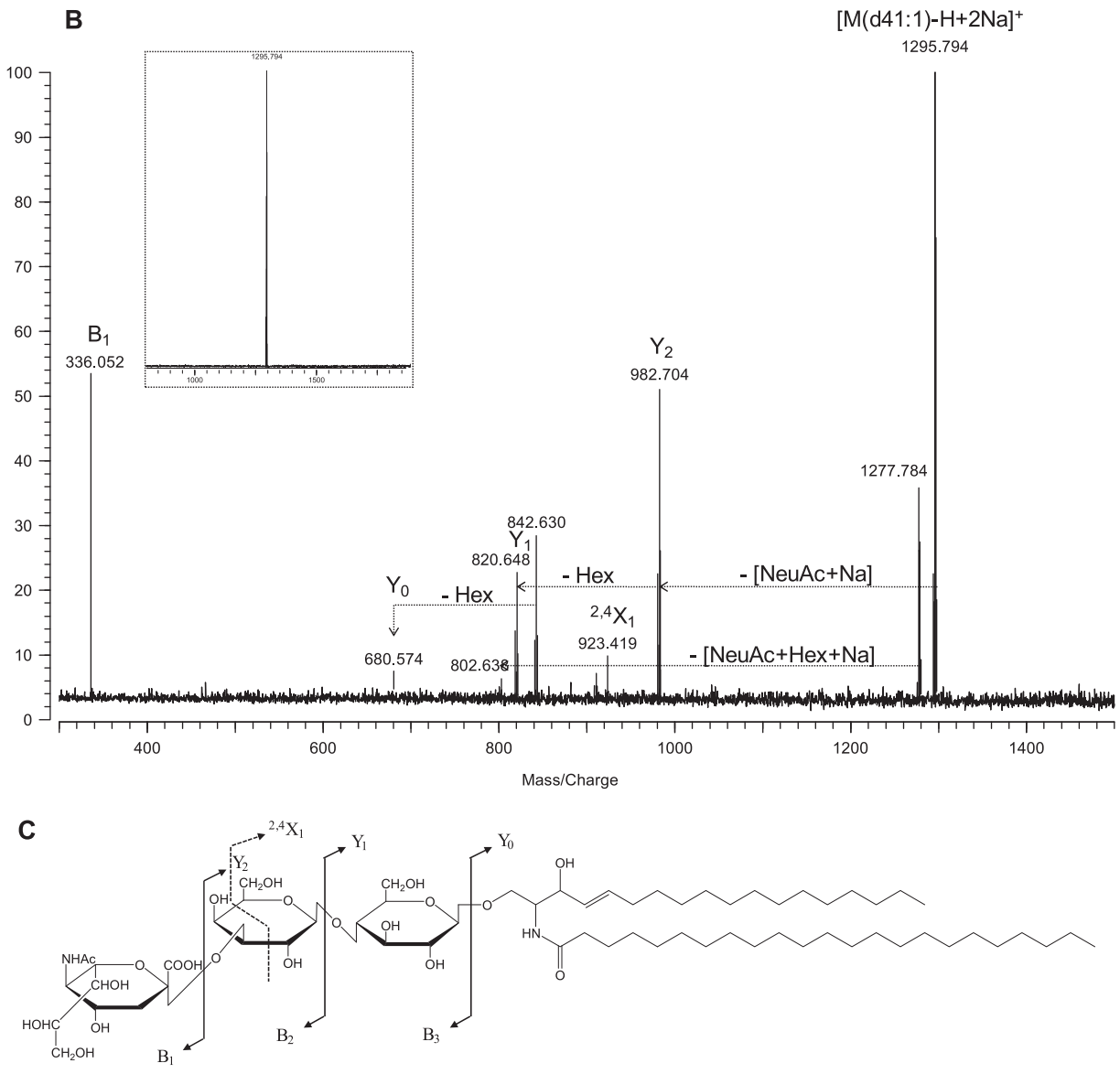

Fig. 3. (*Continued*).

glycopeptides, and glycosphingolipids. For the gangliosides, both positive and negative modes provided extensive fragmentation and produced complimentary information [17,30,38]. In this study, positive mode provides more characteristic fragment ions relating to both glycan and ceramide structures. Fig. 3A shows the product ion spectrum obtained from the CID tandem MS of the GM3(d41:1) precursor ions ($[M(d41:1)-H+2Na]^+$, *m/z* 1295.794) in the positive mode. The quasimolecular ion yields the loss in sequence of one NeuAc at *m/z* 982.717 and one hexose at *m/z* 820.657. The B_2 ion and loss of NeuAc indicate the position of NeuAc at the non-reducing end. Loss of one NeuAc and two hexoses leaves the ceramide ion at *m/z* 680.582 as a di-sodiated form. In the IRMPD tandem MS spectrum (Fig. 3B), the precursor ion was clearly observed. The monosaccharide sequence was readily determined by consecutive loss of NeuAc and two hexoses. Cross-ring cleavage of the oligosaccharide moiety yielded information regarding the linkage. Distinct fragments were reported depending on their terminal structures [39,40]. In this study, X-type ring cleavage ion was observed at *m/z* 923.431. The $^{2,4}X_1$ ion suggests that the terminal NeuAc was linked to the hexose either via 2,3 linkage and not the alternative of 2,6.

The CID of the isolated GD3(d41:1) at *m/z* 1608.872 is shown in Fig. 4A. CID yields the loss of one NeuAc at *m/z* 1295.795, followed by the loss of a second NeuAc at *m/z* 982.717, and the loss of a hexose at *m/z* 820.664. The fragment ion resulting from the cleavage of one NeuAc from the intact molecule was detected as sodiated form at *m/z* 1295.795, along with its counterpart ion at *m/z* 336.067 arising from the non-reducing end. The ion at *m/z* 982.717 was generated by the loss of the 2NeuAc from the molecular ion. The disialo group is documented by the fairly abundant ion at *m/z* 649.144, detected at high mass accuracy. However, complete oligosaccharide fragmentation could not be obtained in a single tandem MS event. IRMPD generally produced fewer fragment ions than CID (Fig. 4B). Y_2 ion at *m/z* 982.717 shows the loss of 2NeuAc, while B_1/B_2 ions indicate the terminal position of two NeuAcs.

3.3. Identification of gangliosides from bovine milk and human milk

To examine biological samples, the negative ion mode was used because it produced the least amount of fragmentation during the

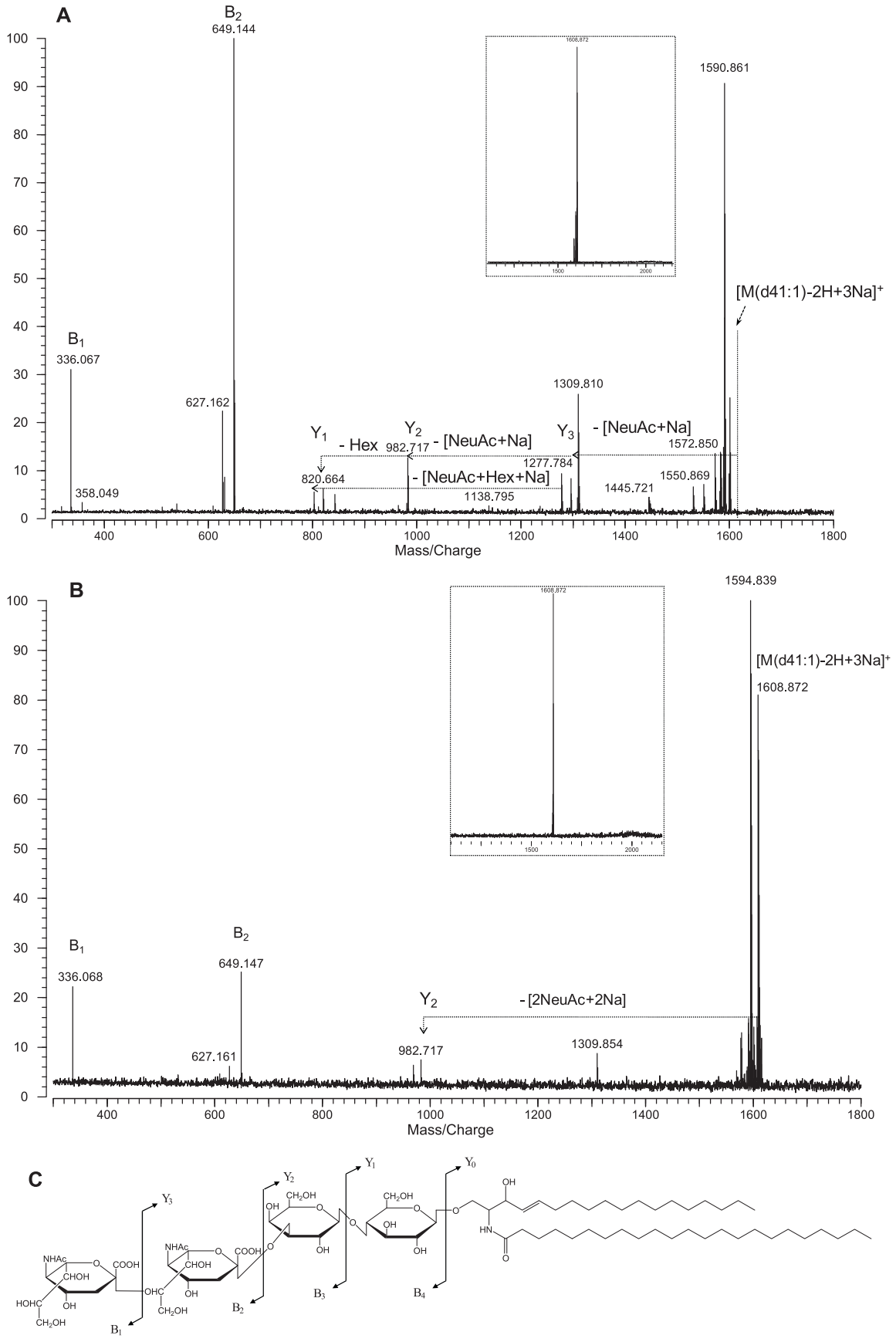

Fig. 4. Tandem MS spectra of ganglioside GD3 from bovine buttermilk in the positive mode using (A) CID and (B) IRMPD with the precursor ion at *m/z* 1608.872. Insets are the isolation of the peak of interest. (C) Fragmentation of the GD3 species detected at *m/z* 1608.872. The structure depicted refers to GD3 known as a dominant form in bovine milk.

Table 1
Tentative assignments of milk gangliosides. (A) Bovine milk and (B) human milk. Assignments are based on accurate masses and tandem MS. Only monoisotopic masses are considered for assignments. Monoisotopic *m/z* values of ions are given.

Type of molecular ion	Predicted *m/z*	Observed *m/z*	Error (ppm)	Assigned structure
A				
$[M-H]^-$	1207.768	1207.772	−3.6	GM3(d38:l)
$[M-H]^-$	1221.784	1221.789	−4.7	GM3(d39:l)
$[M-H]^-$	1235.799	1235.801	−1.0	GM3(d40:l)
$[M-H]^-$	1249.815	1249.815	0.0	GM3(d41:l)
$[M-H]^-$	1261.815	1261.820	−3.9	GM3(d42:2)
$[M-H]^-$	1263.831	1263.830	0.6	GM3(d42:l)
$[M-H]^-$	1277.846	1277.852	−4.5	GM3(d43:l)
$[M-H_2O-H]^-$	1494.868	1494.876	−4.9	GD3(d39:l)
$[M-H_2O-H]^-$	1508.884	1508.885	−0.3	GD3(d40:l)
$[M-H_2O-H]^-$	1522.900	1522.900	0.0	GD3(d41:l)
$[M-H]^-$	1526.895	1526.896	−1.0	GD3(d40:l)
$[M-H_2O-H]^-$	1534.900	1534.902	−1.2	GD3(d42:2)
$[M-H_2O-H]^-$	1536.915	1536.914	1.2	GD3(d42:l)
$[M-H]^-$	1540.910	1540.912	−1.0	GD3(d41:l)
$[M+Na-2H]^-$	1548.877	1548.882	−3.2	GD3(d40:l)
$[M-H]^-$	1552.910	1552.914	−2.1	GD3(d42:2)
$[M-H]^-$	1554.926	1554.926	−0.3	GD3(d42:l)
$[M+Na-2H]^-$	1562.892	1562.899	−4.4	GD3(d41:l)
$[M-H]^-$	1568.942	1568.950	−5.1	GD3(d43:l)
$[M+Na-2H]^-$	1576.908	1576.913	−2.9	GD3(d42:l)
$[M-H]^-$	1966.064	1966.070	−3.3	NeuAc:2HexNAc:4Hex–Cer(d40:l)[a]
$[M-H]^-$	1980.079	1980.086	−3.4	NeuAc:2HexNAc:4Hex–Cer(d41:l)[a]
$[M-H]^-$	1994.095	1994.104	−4.7	NeuAc:2HexNAc:4Hex–Cer(d42:l)[a]
B				
$[M-H]^-$	1151.705	1151.709	−3.6	GM3(d34:l)
$[M-H]^-$	1177.721	1177.726	−4.4	GM3(d36:2)
$[M-H]^-$	1179.737	1179.738	−1.3	GM3(d36:l)
$[M-H]^-$	1205.752	1205.756	−2.7	GM3(d38:2)
$[M-H]^-$	1207.768	1207.770	−1.7	GM3(d38:l)
$[M-H]^-$	1233.784	1233.787	−2.5	GM3(d40:2)
$[M-H]^-$	1235.799	1235.799	0.0	GM3(d40:l)
$[M-H]^-$	1259.799	1259.801	−1.5	GM3(d42:3)
$[M-H]^-$	1261.815	1261.816	−0.9	GM3(d42:2)
$[M-H]^-$	1263.831	1263.831	−0.2	GM3(d42:l)
$[M-H]^-$	1470.832	1470.830	1.3	GD3(d36:l)
$[M-H]^-$	1498.863	1498.860	2.0	GD3(d38:l)
$[M-H_2O-H]^-$	1508.884	1508.884	0.0	GD3(d40:l)
$[M+Na-2H]^-$	1520.845	1520.840	3.6	GD3(d38:l)
$[M-H]^-$	1524.879	1524.875	2.5	GD3(d40:2)
$[M-H]^-$	1526.895	1526.889	3.7	GD3(d40:l)
$[M-H_2O-H]^-$	1536.915	1536.909	4.2	GD3(d42:l)
$[M+Na-2H]^-$	1548.877	1548.876	0.7	GD3(d40:l)
$[M-H]^-$	1552.910	1552.907	2.0	GD3(d42:2)
$[M-H]^-$	1554.926	1554.919	4.3	GD3(d42:l)

[a] Composition was only determined by exact mass measurements.

MALDI process. While there are methods to decrease the fragmentation, they often require additional efforts that defeat the concept of rapid profiling [18,19,25,26]. We chose to accept some fragmentation because the degree of fragmentation is generally consistent under identical ionization conditions and can be readily accounted for in the analysis.

Gangliosides were extracted from bovine and human milk, and the samples were analyzed in the negative ion mode under the same experimental conditions. MS data were interpreted with the use of both accurate mass measurement and Kendrick mass defect (KMD) methods. The analysis of the ganglioside fractions from the milk shows the mass distributions that we identified as NeuAc–2Hex–Cer (GM3) that range from *m/z* 1152 to 1278 and 2NeuAc–2Hex–Cer (GD3) that range from *m/z* 1471 to 1577. Fifteen and 16 gangliosides were observed in bovine and human milk, respectively. In Table 1, assignment of an ion to a certain composition was made on the basis of MALDI FTICR MS spectra by the exact mass calculation (Fig. 5). Less than 5 ppm mass errors were routinely obtained from a two-point calibration with internal standards. The most abundant ions are assigned to $[GM3(d42:1)-H]^-$, $[GD3(d42:1)-H_2O-H]^-$ and $[GM3(d40:1)-H]^-$. Other gangliosides exhibiting a high degree of heterogeneity in their ceramide motifs are also detected as intense ions. In bovine milk, seven different molecular variants of GM3 and six variants of GD3 were detected. Ten GM3 variants and six GD3 variants were detected as fairly abundant ions in human milk gangliosides.

The identities of the gangliosides in the spectra were further validated by data interpretation techniques using KMD plots. We have recently used this method to examine lipids and assign structural classes in complex mixtures [41]. In the *m/z* 1000–2000 range, the monoisotopic peaks in each mass spectrum were processed by KMD analysis in order to group each ganglioside according to its substructure (Fig. 6) [36,37]. Three clusters were observed in the KMD plot from milk ganglioside spectra. The grouping of ions into distinct regions is expected for each of the ganglioside species, and outlined groups are assigned based on the data from Table 1. Compounds with identical KMD values represent the members of a CH_2 homologous series and are easily discerned from the plot as a straight line parallel to the *x*-axis in the plot. In the GM3 group, the points fall on three horizontal lines differing by 0.013, which indicates that there are three different degrees of unsaturation in the ceramide portion of bovine milk gangliosides (Fig. 6B) [41]. In the case of GD3, in one cluster, three types of quasimolecular ions, $[M-H_2O-H]^-$, $[M-H]^-$ and $[M+Na-2H]^-$ varied slightly in

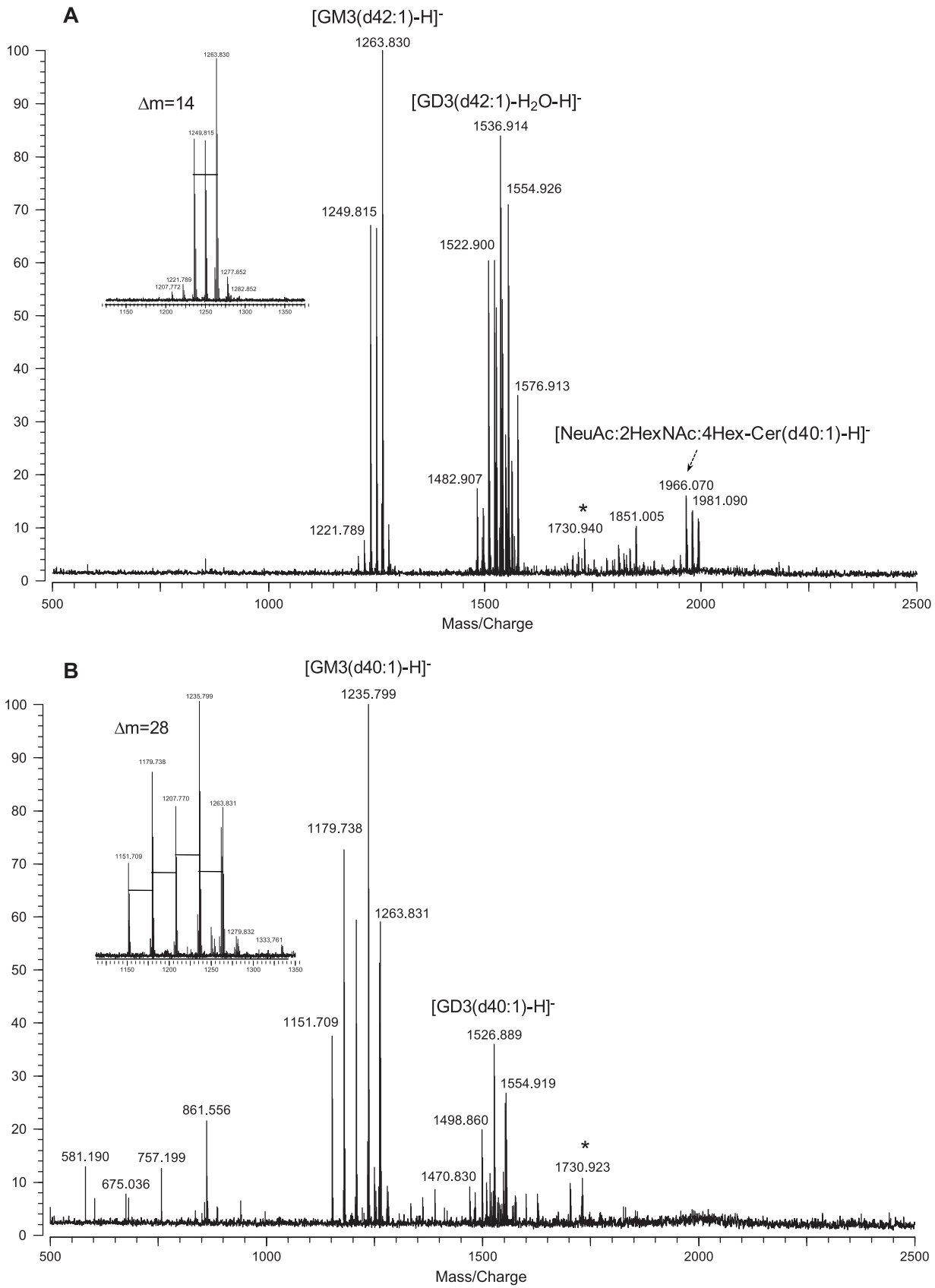

Fig. 5. Representative MALDI-MS spectra of gangliosides from bovine and human milk. Negative mode MALDI-MS spectrum of (A) bovine milk gangliosides and (B) human milk gangliosides. Enlarged spectrum shows the ceramide heterogeneities of ganglioside GM3 species.

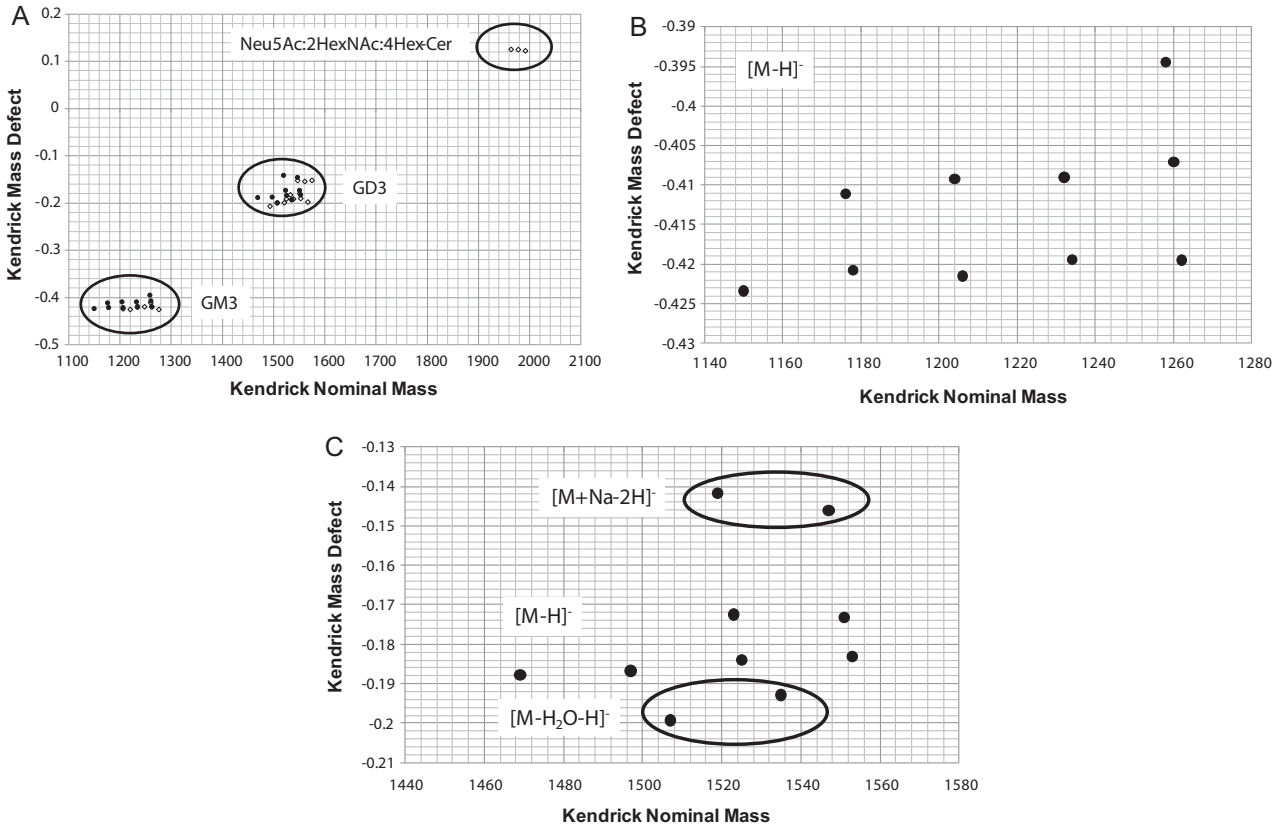

Fig. 6. Kendrick mass defect analysis of milk gangliosides. (◊) Bovine milk ganglioside; (●) human milk ganglioside. (A) Kendrick mass plot, (B) GM3 cluster from human milk ganglioside, and (C) GD3 cluster from human milk ganglioside. Grouping of ions into distinct regions is shown in the Kendrick mass plot, and each cluster has several different degrees of unsaturation.

their positions [42]. Two different degrees of unsaturation were observed from deprotonated forms (Fig. 6C) (Table 2).

In the case of bovine milk, in addition to GM3 and GD3, other gangliosides were observed at *m/z* 1966.070, 1980.086, and 1994.104. Their mass intervals, 14.02, imply alkyl chains, and the type of quasimolecular ion $[M-H]^-$ implies that the compounds each have only one sialic acid. With the assumption that the compositions of the ceramides are d40:1, d41:1, and d42:1, which are the backbone ceramides of bovine milk GM3 and GD3, from them, the oligosaccharides were assigned as 1NeuAc + 2HexNac + 4Hex. These findings are consistent with a previously reported bovine milk monosialoganglioside, the structure of which is Galβ1–4GalNAcβ1–6(NeuAcα2–6Galβ1–4GalNAcβ1–3)Galβ1–4Glcβ–Cer [34].

Oligosaccharide sequences were further determined by tandem MS. Fragmentation patterns were similar with those described previously for the standard. For example, CID MS/MS was achieved with NeuAc–2Hex–Cer(d40:1) at *m/z* 1281.779 as a precursor ion to confirm the oligosaccharide sequence of human milk gangliosides (Suppl. 3). Consecutive loss of NeuAc and hexose was observed. Along with the postulation of core structures, the sequences of two major gangliosides were NeuAc–Hex–Hex–Cer and NeuAc–NeuAc–Hex–Hex–Cer [1]. They correspond to GM3 and GD3, respectively, which were consistent with previously described structures [43,44]. In this study, GM3 and GD3 from bovine and human milk ganglioside fractions were confirmed by CID and/or IRMPD.

Several differences have been observed between bovine and human milk gangliosides. Even though we needed to take into consideration in-source fragmentation, we observed different ion intensities for each ganglioside species. For example, GD3 species is the most abundant ion in bovine milk gangliosides. Mass spectra also show the differences in the ceramide subspecies. The 14.0 Da and 28.0 Da intervals within the peak clusters can be explained by ceramide variation in the sphingoid base and/or fatty acid, with one or two CH_2 groups, respectively. While observing 14.0 Da intervals in the mass peak clusters in the analysis of bovine milk gangliosides, we observed 28.0 Da intervals in the peak clusters of human milk, which indicate that only human milk gangliosides are the ceramide carbons always even numbered. Interestingly, the high resolving

Table 2
Oligosaccharide and ceramide compositions of major bovine and human milk gangliosides.

	Bovine milk	Human milk
Major oligosaccharide	NeuAc–2Hex–Cer (GM3) 2NeuAc–2Hex–Cer (GD3) NeuAc:2HexNAc:4Hex–Cer	NeuAc–2Hex–Cer (GM3) 2NeuAc–2Hex–Cer (GD3)
Major ceramide	d39:1 d40:1 d41:1 d42:1 d43:1	d34:1 d36:1 d38:1 d40:1 d42:1

power of the FT analyzer makes it possible to determine the number of double bonds, which might vary in ceramide moieties. For example, in human milk, GM3(d42:1) at *m/z* 1263.8307, GM3(d42:2) at *m/z* 1261.8160, and GM3(d42:3) at *m/z* 1259.8012 were observed; thus, they were situated on three different horizontal lines in the KMD plot. They are often not well-observed with the use of MALDI TOF due to the poor resolution of the TOF analyzer [12].

Recently, it has been reported that gangliosides may contribute to immunity and to the prevention of infection [7–9]. Milk gangliosides are known to compete for pathogen binding sites and to block pathogens from binding to their host cell receptors in the mucosa epithelial cell. The specificity of the binding of the different pathogens to their ganglioside receptors is indicative of a heterogeneous approach, with each binding interaction displaying its own specific structure-mediated characteristics [45]. Even though ganglioside binders specifically recognize the oligosaccharide portion of gangliosides, ceramide structures influence their binding specificity and capacity. For example, pathogens show differing binding capacities with respect to molecular species with various levels of hydroxylation and chain length [46,47]. Therefore, the structural differences between human and bovine milk gangliosides probably result in biologically distinct functions, which are not yet understood much less annotated in detail due to the lack of sensitive analytical tools.

4. Conclusions

The present results introduce a rapid means to analyze and characterize milk gangliosides with the use of MALDI FTICR MS coupled with CID and IRMPD MS/MS. Its high resolving power and mass accuracy provides detailed compositional information. Oligosaccharide sequences of ganglioside GM3 and GD3 were obtained with the use of tandem mass spectrometry. Major differences in the abundance of each species and the ceramide distributions were observed in bovine and human milk gangliosides, respectively. Mass spectrometry successfully provided structure information of both the polar head group and the ceramide backbone with a more comprehensive description of ganglioside profiles, details necessary to broadening our knowledge of the biological structure–function relationships of complex milk gangliosides. This method can provide complementary information when combined with traditional TLC and immunological methods.

Acknowledgments

The authors acknowledge all the students, postdocs, and staff in the UC Davis Milk Bioactives Program (http://mbp.ucdavis.edu) and Functional Glycobiology Program (http://fgp.ucdavis.edu). The authors are grateful to Jennifer T. Smilowitz for providing the human milk sample. This publication was made possible in part by grant support from the University of California Discovery Grant Program, the California Dairy Research Foundation, Dairy Management Inc., NIEHS Superfund P42 ES02710, the Charge study P01 ES11269, and by NIH-NICID awards 5R01HD059127 and 1R01HD061923.

Appendix A. Supplementary data

Supplementary data associated with this article can be found, in the online version, at doi:10.1016/j.ijms.2010.10.020.

References

[1] A. Varki, Essentials of Glycobiology, 2nd ed., Cold Spring Harbor Laboratory Press, Cold Spring Harbor, NY, 2009.
[2] A.H. Merrill Jr., M.D. Wang, M. Park, M.C. Sullards, (Glyco)sphingolipidology: an amazing challenge and opportunity for systems biology, Trends Biochem. Sci. 32 (2007) 457–468.
[3] R.L. Schnaar, Glycosphingolipids in cell surface recognition, Glycobiology 1 (1991) 477–485.
[4] R. Kannagi, E. Nudelman, S. Hakomori, Possible role of ceramide in defining structure and function of membrane glycolipids, Proc. Natl. Acad. Sci. U.S.A. 79 (1982) 3470–3474.
[5] J.B. German, C.J. Dillard, R.E. Ward, Bioactive components in milk, Curr. Opin. Clin. Nutr. Metab. Care 5 (2002) 653–658.
[6] T.W. Keenan, Composition and synthesis of gangliosides in mammary gland and milk of the bovine, Biochim. Biophys. Acta 337 (1974) 255–270.
[7] D.S. Newburg, G.M. Ruiz-Palacios, A.L. Morrow, Human milk glycans protect infants against enteric pathogens, Annu. Rev. Nutr. 25 (2005) 37–58.
[8] R. Rueda, The role of dietary gangliosides on immunity and the prevention of infection, Br. J. Nutr. 98 (Suppl. 1) (2007) S68–73.
[9] K.A. Karlsson, Animal glycosphingolipids as membrane attachment sites for bacteria, Annu. Rev. Biochem. 58 (1989) 309–350.
[10] F. Sanchez-Juanes, J.M. Alonso, L. Zancada, P. Hueso, Glycosphingolipids from bovine milk and milk fat globule membranes: a comparative study. Adhesion to enterotoxigenic Escherichia coli strains, Biol. Chem. 390 (2009) 31–40.
[11] M. Iwamori, K. Takamizawa, M. Momoeda, Y. Iwamori, Y. Taketani, Gangliosides in human, cow and goat milk, and their abilities as to neutralization of cholera toxin and botulinum type A neurotoxin, Glycoconj. J. 25 (2008) 675–683.
[12] L. Bode, C. Beermann, M. Mank, G. Kohn, G. Boehm, Human and bovine milk gangliosides differ in their fatty acid composition, J. Nutr. 134 (2004) 3016–3020.
[13] M.J. Martin, S. Martin-Sosa, P. Hueso, Bovine milk gangliosides: changes in ceramide moiety with stage of lactation, Lipids 36 (2001) 291–298.
[14] S.B. Levery, Glycosphingolipid structural analysis and glycosphingolipidomics, Methods Enzymol. 405 (2005) 300–369.
[15] R.W. Ledeen, R.K. Yu, Gangliosides: structure, isolation, and analysis, Methods Enzymol. 83 (1982) 139–191.
[16] D.J. Harvey, Analysis of carbohydrates and glycoconjugates by matrix-assisted laser desorption/ionization mass spectrometry: an update for the period 2005–2006, Mass Spectrom. Rev. (2010).
[17] Y. Park, C.B. Lebrilla, Application of Fourier transform ion cyclotron resonance mass spectrometry to oligosaccharides, Mass Spectrom. Rev. 24 (2005) 232–264.
[18] P. Juhasz, C.E. Costello, Matrix-assisted laser desorption ionization time-of-flight mass spectrometry of underivatized and permethylated gangliosides, J. Am. Soc. Mass Spectrom. 3 (1992) 785–796.
[19] S.G. Penn, M.T. Cancilla, M.K. Green, C.B. Lebrilla, Direct comparison of matrix-assisted laser desorption/ionization and electrospray ionisation in the analysis of gangliosides by Fourier transform mass spectrometry, Eur. Mass Spectrom. 3 (1997) 67–79.
[20] A.K. Powell, D.J. Harvey, Stabilization of sialic acids in N-linked oligosaccharides and gangliosides for analysis by positive ion matrix-assisted laser desorption/ionization mass spectrometry, Rapid Commun. Mass Spectrom. 10 (1996) 1027–1032.
[21] D.J. Harvey, Matrix-assisted laser desorption/ionization mass spectrometry of sphingo- and glycosphingo-lipids, J. Mass Spectrom. 30 (1995) 1311–1324.
[22] D.J. Harvey, Matrix-assisted laser desorption/ionization mass spectrometry of carbohydrates, Mass Spectrom. Rev. 18 (1999) 349–450.
[23] J.B. German, L.A. Gillies, J.T. Smilowitz, A.M. Zivkovic, S.M. Watkins, Lipidomics and lipid profiling in metabolomics, Curr. Opin. Lipidol. 18 (2007) 66–71, doi:10.1097/MOL.1090b1013e328012d328911.
[24] M. Ishida, T. Yamazaki, T. Houjou, M. Imagawa, A. Harada, K. Inoue, R. Taguchi, High-resolution analysis by nano-electrospray ionization Fourier transform ion cyclotron resonance mass spectrometry for the identification of molecular species of phospholipids and their oxidized metabolites, Rapid Commun. Mass Spectrom. 18 (2004) 2486–2494.
[25] P.B. O'Connor, C.E. Costello, A high pressure matrix-assisted laser desorption/ionization Fourier transform mass spectrometry ion source for thermal stabilization of labile biomolecules, Rapid Commun. Mass Spectrom. 15 (2001) 1862–1868.
[26] P.B. O'Connor, E. Mirgorodskaya, C.E. Costello, High pressure matrix-assisted laser desorption/ionization Fourier transform mass spectrometry for minimization of ganglioside fragmentation, J. Am. Soc. Mass Spectrom. 13 (2002) 402–407.
[27] V.B. Ivleva, Y.N. Elkin, B.A. Budnik, S.C. Moyer, P.B. O'Connor, C.E. Costello, Coupling thin-layer chromatography with vibrational cooling matrix-assisted laser desorption/ionization Fourier transform mass spectrometry for the analysis of ganglioside mixtures, Anal. Chem. 76 (2004) 6484–6491.
[28] C.E. Costello, J.E. Vath, Tandem mass spectrometry of glycolipids, Methods Enzymol. 193 (1990) 738–768.
[29] T. Ii, Y. Ohashi, Y. Nagai, Structural elucidation of underivatized gangliosides by electrospray-ionization tandem mass spectrometry (ESIMS/MS), Carbohydr. Res. 273 (1995) 27–40.
[30] M.A. McFarland, A.G. Marshall, C.L. Hendrickson, C.L. Nilsson, P. Fredman, J.E. Mansson, Structural characterization of the GM1 ganglioside by infrared multiphoton dissociation, electron capture dissociation, and electron detachment dissociation electrospray ionization FT-ICR MS/MS, J. Am. Soc. Mass Spectrom. 16 (2005) 752–762.
[31] L. Svennerholm, Chromatographic separation of human brain gangliosides, J. Neurochem. 10 (1963) 613–623.
[32] B. Domon, C.E. Costello, A systematic nomenclature for carbohydrate fragmentations in FAB-MS/MS spectra of glycoconjugates, Glycoconj. J. 5 (1988) 397–409.

[33] D.F. Smith, P.A. Prieto, Special considerations for glycolipids and their purification, Curr. Protoc. Mol. Biol. (2001) (Unit 17 13, Chapter 17).
[34] K. Takamizawa, M. Iwamori, M. Mutai, Y. Nagai, Gangliosides of bovine buttermilk. Isolation and characterization of a novel monosialoganglioside with a new branching structure, J. Biol. Chem. 261 (1986) 5625–5630.
[35] B.H. Clowers, E.D. Dodds, R.R. Seipert, C.B. Lebrilla, Dual polarity accurate mass calibration for electrospray ionization and matrix-assisted laser desorption/ionization mass spectrometry using maltooligosaccharides, Anal. Biochem. 381 (2008) 205–213.
[36] C.A. Hughey, C.L. Hendrickson, R.P. Rodgers, A.G. Marshall, K. Qian, Kendrick mass defect spectrum: a compact visual analysis for ultrahigh-resolution broadband mass spectra, Anal. Chem. 73 (2001) 4676–4681.
[37] E. Kendrick, A mass scale based on CH_2 = 14.0000 for high resolution mass spectrometry of organic compounds, Anal. Chem. 35 (1963) 2146–2154.
[38] D.J. Harvey, Proteomic analysis of glycosylation: structural determination of N- and O-linked glycans by mass spectrometry, Expert Rev. Proteom. 2 (2005) 87–101.
[39] S.F. Wheeler, D.J. Harvey, Negative ion mass spectrometry of sialylated carbohydrates: discrimination of N-acetylneuraminic acid linkages by MALDI-TOF and ESI-TOF mass spectrometry, Anal. Chem. 72 (2000) 5027–5039.
[40] I. Meisen, J. Peter-Katalinic, J. Muthing, Discrimination of neolacto-series gangliosides with alpha2-3- and alpha2-6-linked N-acetylneuraminic acid by nanoelectrospray ionization low-energy collision-induced dissociation tandem quadrupole TOF MS, Anal. Chem. 75 (2003) 5719–5725.
[41] L.A. Lerno Jr., J.B. German, C.B. Lebrilla, Method for the identification of lipid classes based on referenced Kendrick mass analysis, Anal. Chem. 82 (2010) 4236–4245.
[42] J.J. Jones, M.J. Stump, R.C. Fleming, J.O. Lay Jr., C.L. Wilkins, Strategies and data analysis techniques for lipid and phospholipid chemistry elucidation by intact cell MALDI-FTMS, J. Am. Soc. Mass Spectrom. 15 (2004) 1665–1674.
[43] R.G. Jensen, D.S. Newburg, Bovine milk lipids, in: G.J. Robert (Ed.), Handbook of Milk Composition, Academic Press, San Diego, 1995, pp. 543–575.
[44] T.W. Keenan, S. Patton, The milk lipid globule membrane, in: G.J. Robert (Ed.), Handbook of Milk Composition, Academic Press, San Diego, 1995, pp. 5–50.
[45] T.L. Gioannini, J.P. Weiss, Regulation of interactions of Gram-negative bacterial endotoxins with mammalian cells, Immunol. Res. 39 (2007) 249–260.
[46] N. Stromberg, K.A. Karlsson, Characterization of the binding of propionibacterium granulosum to glycosphingolipids adsorbed on surfaces. An apparent recognition of lactose which is dependent on the ceramide structure, J. Biol. Chem. 265 (1990) 11244–11250.
[47] M.J. Martin, S. Martin-Sosa, J.M. Alonso, P. Hueso, Enterotoxigenic Escherichia coli strains bind bovine milk gangliosides in a ceramide-dependent process, Lipids 38 (2003) 761–768.